
INTERNATIONAL JOURNAL OF CURRENT RESEARCH IN CHEMISTRY AND PHARMACEUTICAL SCIENCES

(p-ISSN: 2348-5213; e-ISSN: 2348-5221)

www.ijercps.com

(A Peer Reviewed, Referred, Indexed and Open Access Journal)

DOI: 10.22192/ijercps

Coden: IJCROO(USA)

Volume 10, Issue 11- 2023

Research Article



DOI: <http://dx.doi.org/10.22192/ijercps.2023.10.11.001>

Growth, spectral and thermal characterization of anilinium trichloromercurate(II) crystal

G.Raja¹ and T.Dhanabal^{2*}

¹Department of Chemistry, Paavai Engineering College (Autonomous), Namakkal-637 018, Tamil Nadu, India.

²Department of Chemistry, Muthayammal College of Engineering, Rasipuram, Namakkal-637 408, Tamil Nadu, India.

*Corresponding Author: ghanabal27@gmail.com

Abstract

A new semiorganic crystal anilinium trichloromercurate(II) grown by slow evaporation solution growth method. The elemental analysis confirms the stoichiometric of the crystal. The crystalline nature of the crystal was confirmed powder X-ray diffraction pattern. There is no absorption between 330 nm to 800 nm indicates that the grown crystal can be used for optoelectronic applications. The thermal stability of the crystal was performed by TG-DTG and DTA analyses. The FTIR spectrum of the title material characterizes the various characteristics chemical bondings in the crystal. The NLO property of the crystal indicates that the emission of green light confirms the crystal possesses SHG efficiency. The DFT calculation study was studied to find out the HOMO–LUMO energy gap and intra-molecular charge transfer (ICT) interaction occurs within the molecule. The grown crystal exhibits good antibacterial and antifungal activities.

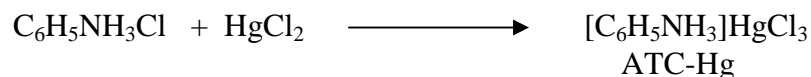
Keywords: Solution growth, Crystal, Thermogravimetric analysis, FTIR spectrum, Optical property.

1.Introduction

The nonlinear optical crystals have been given much importance, because of their potential applications such as telecommunication, optical information process, frequency conversion and optical disk data storage (Lin et al. 1989; Duo-rong et. al. 1996; Masilamani et. al. 2012) Organic crystals show prominent properties due to their fast and nonlinear response. Over a broad frequency

range, they have not only inherent synthetic flexibility and large optical damage threshold, but also have some inherent drawbacks, such as volatility, low thermal stability, and weak mechanical strength. Organic NLO crystals exhibiting better NLO efficiency with poor mechanical, chemical and thermal stability, which are not suitable for device applications. By adding organic counterparts in organic and by increasing second order hyperpolarizability furthermore as a

semiorganic suitable for device fabrication. Incorporating more and new strategies in both organic and inorganic materials leads the birth of semiorganic material (Chemla et. al. 1987; Newman et. al. 1990; Malik et. al. 1999). This semiorganic possess higher NLO efficiency due to their good linear and nonlinear optical activity, chemical flexibility, better hardness values and elevated thermal stability (Johnson et. al. 2019). For the above causes, the researchers are more concentrated in growing the semi organic NLO crystals, which unite the properties of organic and inorganic properties like high laser damage threshold, chemical stability, high transparency and higher chemical strength, which is suitable for the device fabrication (Kennedy et. al. 2014; Hemalatha et. al. 2019; Indumathi et. al. 2021). Most of the organic NLO crystals are constituted by weak van der Waals and hydrogen bonds. So they are soft in nature and it is difficult to cut and polish the crystal due to its softness (Pal et. al. 20002). The mechanical strength of organic crystal is very low. Pure inorganic NLO materials typically have excellent mechanical and thermal properties but possess relatively modest optical nonlinearities because of the lack of extended pi-electron delocalization. The complex of organic-inorganic gives semi-organic material, which possesses



Bright, transparent and brown coloured crystals were harvested in about 20 days under the experimental conditions. Once the crystals were formed, they were carefully collected from the

2.2. Physio-chemical characterization techniques

The elemental analysis of the crystal is recorded at using Vario EL III CHNS instrument at Sophisticated Test and Instrumentation Centre, Cochin University of Science and Technology, Cochin. The powder XRD patterns of ATC-Hg crystal was obtained using BRUKER AXS D8 Advance X-ray diffractometer model instrument with Cu K radiation ($\lambda = 1.54060 \text{ \AA}$) in room temperature at STIC (Sophisticated Test and Instrumentation Centre) Cochin. The UV-visible spectrum is recorded at using JASCO V-670 Spectrophotometer Series instrument at VIT

higher mechanical strength compared to organic materials (Anwar et. al. 2000). Based on the above fact, the most of the semiorganic crystal play vital role in optoelectronic applications.

In this article we have reported the synthesis and characterization of anilinium trichloromercurate(II) $[\text{C}_6\text{H}_5\text{NH}_3]\text{HgCl}_3$ crystals (hereafter abbreviated as (ATC-Hg). The synthesized crystal analyzed through CHNS, PXRD, UV-visible, TG-DTG, DTA, FTIR, NLO, DFT and antimicrobial studies.

2. Materials and Methods

2.1 Growth of ATC-Hg single crystal

The single crystals of anilinium trichloromercurate(II), $[\text{C}_6\text{H}_5\text{NH}_3]\text{HgCl}_3$, were grown by slow evaporation of saturated aqueous solution at room temperature. The compound is abbreviated as ATC-Hg. Aniline hydrochloride and mercuric chloride were separately dissolved in 1:1 molar ratio respectively in triply distilled water. The two solutions were mixed thoroughly and filtered through Whatmann 41 filter paper. The solution in the beaker was covered by an ordinary filter paper and was kept aside. The experimental set up used for growing the crystal is shown in Fig.1. The following chemical equation describes the formation of the crystal.

solution using a well-cleaned forceps. The harvested crystals were recrystallized repeatedly to get crystals of good quality.

University, Vellore. The thermal analyses (TG and DTA) were recorded at STIC, Cochin using a PERKIN ELMER DIAMOND thermal analyzer under nitrogen atmosphere. The sample was heated from room temperature to 1020°C at a heating rate of 10°C per minute. The FTIR spectra of the crystal were recorded at SRMV College of Arts and Science, Coimbatore using a Perkin Elmer model RX1 instrument. The second harmonic generation efficiencies of the crystal were carried out by modified Kurtz-Perry powder technique using Nd:YAG laser, IISc, Bangaluru. The DFT study of the crystal was studied by quantum chemical

descriptors. The antimicrobial studies of the crystal were studied by agar disc diffusion method.

2.3 Antimicrobial activity study

2.3.1 Preparation of chemical extract

A small amount (100 µg) of each of the compound was weighed and mixed with 1ml of the DMSO solvent. The filtrate was obtained by filtration using a Whatman No.1 filter paper. The discs were kept in test tubes containing compound. Then the discs were allowed to dry in laminar airflow chamber. Control was maintained by adding DMSO solvent on the discs.

2.3.2 Antibacterial activity

The antibacterial activity of newly synthesized compound was tested *in vitro* against four Gram-positive bacteria *Staphylococcus epidermidis*, *Staphylococcus aureus* (Lab isolate), *Enterococcus faecalis* and *Staphylococcus aureus* (Clinical isolate) and five Gram-negative bacteria *Proteus sp.*, *Escherichia coli*, *Pseudomonas aeruginosa*, *Pseudomonas sp.* and *Klebsiella pneumoniae* (Guru et. al 2010; Vimalan et. al. 2010). Dimethyl sulphoxide (DMSO) solvent was used as control for all the media. The discs measuring 5 mm in diameter were prepared from Whatman No.1 filter paper sterilized by dry heat at 140°C for 1 h. The sterile discs previously soaked in concentration (100 µg/ml) of the test compound was placed in a nutrient agar medium. The petri plates were inverted and kept in an incubator for 24 h at 37°C. Tetracycline (30 mg/disc, Hi-Media) was used as a standard drug. To obtain the diameter of zone, 0.1 ml volume of each sample was taken and spread on agar plates. The number of colony forming units (cfu) was counted after 24 h of incubation at 35°C.

Table 1. Elemental analysis data of ATC-Hg crystal.

Element	Carbon %	Hydrogen %	Nitrogen %
Experimental	18.49	2.04	3.39
Calculated	17.94	2.01	3.49

3.2. Powder X-ray diffraction method

After incubation the zone of inhibition was measured and expressed as mm.

2.3.3 Antifungal activity

The newly synthesized compound was also screened for their antifungal activity against *Aspergillus niger*, *Aspergillus flavus*, *Aspergillus fumigatus*, *Candida albicans* and *Penicillium sp.* in DMSO solvent by using standard agar disc diffusion method. The synthesized compound was dissolved in DMSO solvent which was used as control for all the media. All cultures were routinely maintained on Sabourauds dextrose agar (SDA) and incubated at 28°C. Spore formation of filamentous fungi was formed from seven days old culture on sterile normal solution, which was diluted to obtain approximately, 10⁵ cfu/ml. The culture was centrifuged at 1000 rpm, pellets were resuspended and diluted in sterile non-sterilized saline (NSS) to obtain a viable count 10⁵ cfu/ml. With the help of spreader, 0.1 ml volume of diluted fungal culture suspension was taken and spread on agar plates. The fungal activity of compound was compared with Nystatin (30 g/disc Hi-Media) as a standard drug. The cultures were incubated for 48 h at 37°C and the growth was monitored. The inhibition zone was determined by measuring the diameters of the zone (mm).

3. Results and discussion

3.1. Elemental analysis

The elemental analysis data obtained for ATC-Hg crystal is given in Table 1. The experimental values of carbon, nitrogen and hydrogen percentages are very close to the theoretical values. This confirms that the crystal is formed in the stoichiometric ratio.

The experimental and stimulated powder XRD pattern of ATC-Hg crystals is shown in Figure 1. The experimental 2θ , d and I values are given in Table 2. The sharp and well defined Bragg peaks at specific 2θ values in the powder XRD pattern confirm the crystalline nature of the crystal. The title is indexed using CRYSFIRE software. The crystal belongs to monoclinic system with cell parameters, $a = 13.6170\text{\AA}$, $b = 14.3456\text{\AA}$, $c = 8.5140\text{\AA}$ and $\alpha = 90^\circ$, $\beta = 102.10^\circ$ and $\gamma = 90^\circ$. The unit cell volume is 1971.91\AA^3 . The compound

HgCl_2 belongs to orthorhombic system. The crystal system of the synthesized crystal, ATC-Hg is entirely different from HgCl_2 crystal system that

indicates the formation of ATC-Hg crystal. The high sharp peak in the PXRD pattern indicates the crystalline nature and quality of the crystal.

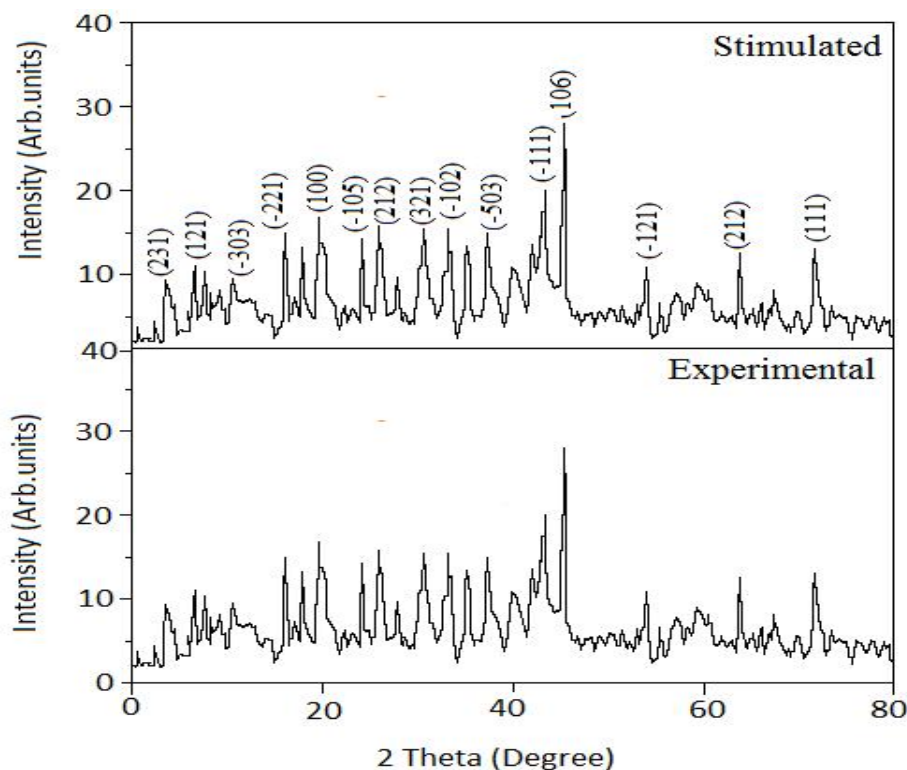


Figure 2. Experimental and simulated powder XRD pattern of the ATC-Hg crystal.

3.3. UV-Visible spectral study

Transmission spectra are very important for any single crystal which can be useful for any practical application, only if it has a wide transparency window. The UV-visible Transmission spectrum and photograph (inserted) of ATC-Hg crystal is

shown in Figure 2. The absorption peaks observed at 240 nm and 280 nm are due to electronic transitions. There is no absorption between 300 nm and 1200 nm. Hence it is a potential contender for nonlinear optical applications. The transmittance between 350 and 800 nm is approximately 70%.

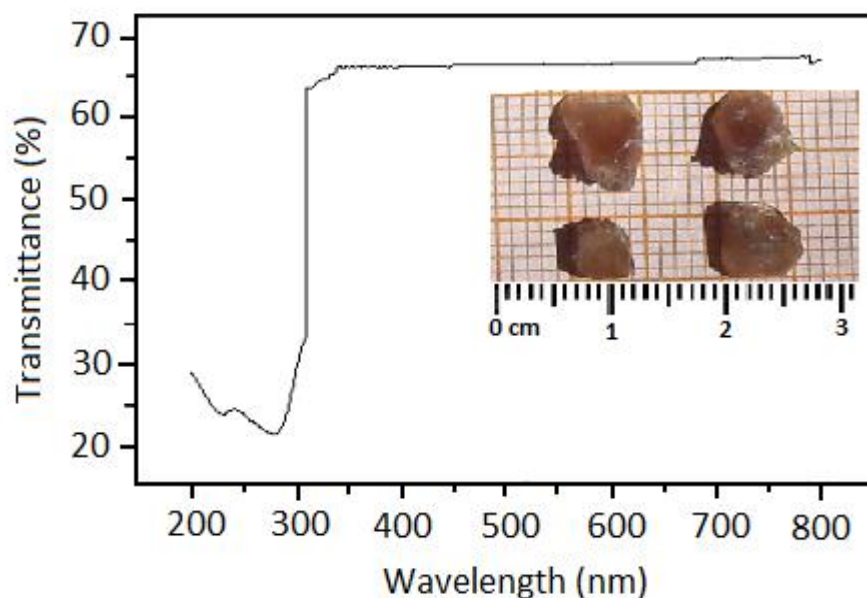


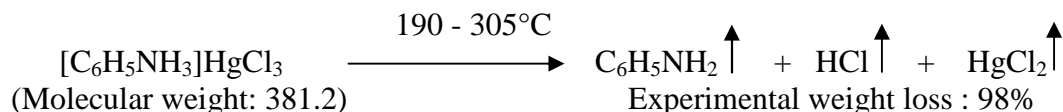
Figure 3. UV-visible spectrum and photograph (inserted) of ATC-Hg crystal.

3.4. Thermal analyses

3.4.1. Thermogravimetric Analysis

The TGA thermogram of the ATC-Hg is shown in Figure 3. The compound is subjected to a uniform heating at a heating rate of 25°C per minute under nitrogen atmosphere. When the sample is heated from room temperature to 800°C, a prolonged decomposition starts at 190°C and extends upto 305°C. The TG thermogram shown in Figure 6 shows a single stage weight loss in this compound.

The thermogram shows a weight loss of 98% between 190 and 305°C. This is due to the loss of aniline, HCl and HgCl₂ molecules. The calculated weight loss is 99.9%. The difference of 1.9% between the calculated and experimental weight losses is due to loss of the adsorbed and occluded water molecules associated with the crystal. The following decomposition pattern has been formulated to account the weight loss. Thus, the TG study confirms the formation of the compound in the stoichiometric ratio.



3.4.2. Differential Thermal Analysis

The DTA curve of the compound ATC-Hg is shown in Figure 4. There are two sharp exothermic peaks. The first exothermic peak at 176°C is close

to the melting of the compound. The melting point of the compound was found to be 172°C. The peak at 260°C and a small hump at 303°C are due to the decomposition of the compound into fragments. Thus the DTA study conforms to TGA.

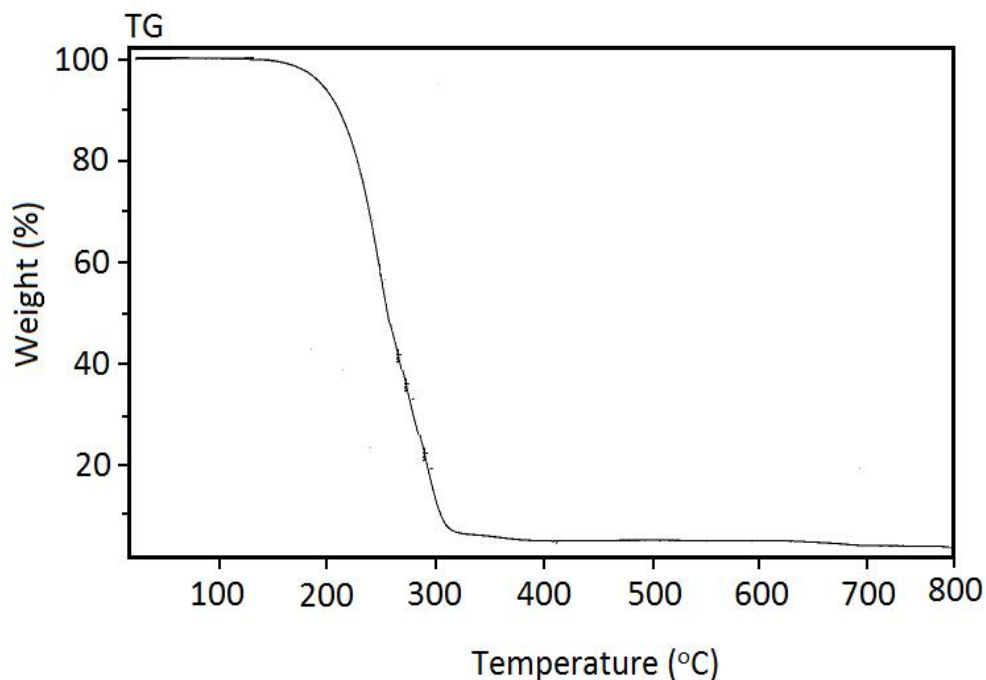


Figure 4. TG thermogram of ATC-Hg crystal.

3.5. FTIR spectroscopic method

The FTIR spectrum of grown ATC-Hg crystals is shown in Figure 5. The broad absorption frequency at 3000cm^{-1} is due to aromatic C-H stretching. The absorption frequency at 3525cm^{-1} is due to O-H stretching and for N-H stretching vibrational modes. The weak frequency observed at 1480cm^{-1} is assigned to C=C stretching in aromatic

hydrocarbon. C-N stretching vibration is found at 1281cm^{-1} . The absorption at 1080cm^{-1} is due to the asymmetric C-C stretching vibration. The absorption at 740cm^{-1} is due to C-C out plane bending in aromatic nucleus. The frequency observed at 463cm^{-1} is due to the HgCl_3^- internal vibrations.

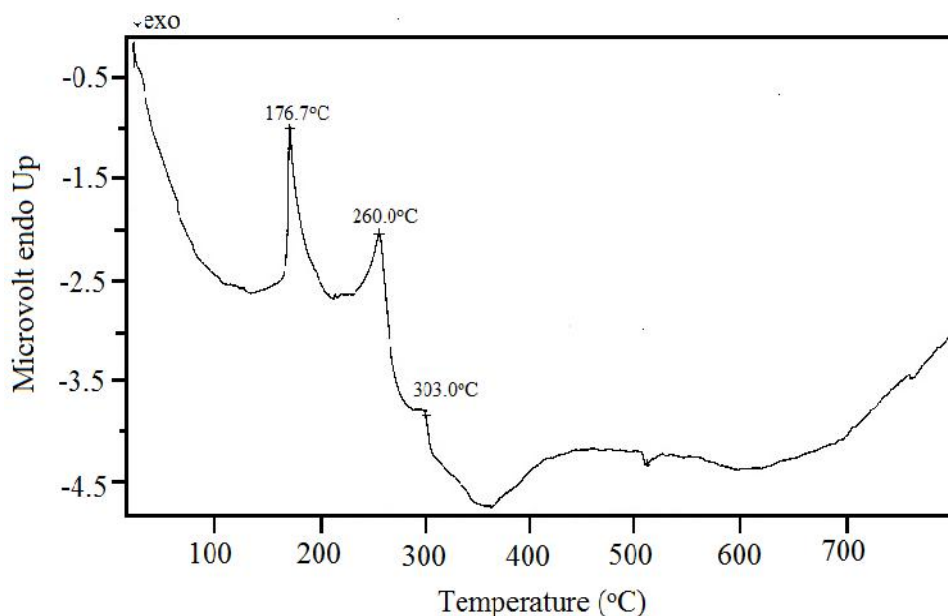


Figure 4. DTA thermogram of ATC-Hg crystal.

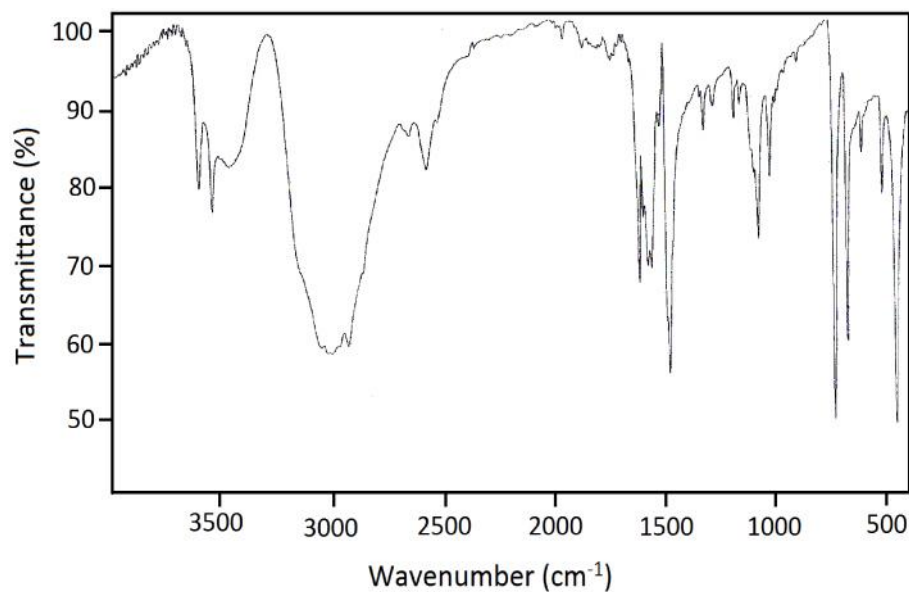


Figure 6. FTIR spectrum of ATC-Hg crystal.

3.6 Non linear optical (NLO) study

The powder SHG efficiency of the crystal was studied using a mode locked Q-switched Nd:YAG laser by employing the modified Kurtz-Perry powder technique (Kurtz and Perry 1968). The fundamental beam of 1064 nm from Q-switched Nd:YAG laser pulse energy 6mJ/s with pulse width of 8 ns and repetition rate of 10 Hz was used to test the second harmonic generation. The output from

Nd:YAG laser was used as illuminating source to the crystal specimen. The output from Q-switched laser was focused onto the crystals. Crystal of ATC-Hg was powered with a uniform particle size and then packed in a microcapillary of uniform bore and exposed to laser radiation. Second harmonic radiation generated by the randomly oriented microcrystals was focused by a lens and detected by a photomultiplier tube. A sample of potassium dihydrogen phosphate (KDP) was used as a

reference material. The emission of green light from the material confirms the material possess NLO activity. The NLO activity of this crystal may be due to intense intermolecular hydrogen bonding within the crystal. SHG efficiency of the grown crystal 0.5 time greater than that Standard KDP.

3.7 DFT study

Density Functional Theory (DFT) of chemical reactivity is known conceptual density functional theory. One of the aims of the conceptual density functional theory is to calculate the quantum

chemical descriptors like hardness (χ), electronegativity (χ) and chemical potential (μ) giving useful hints about the stability of reactivity of chemical species. In this theory, aforementioned quantum chemical descriptors are calculated via following equations including ground state ionization energy and electron affinity values of chemical species (atoms, ions and molecules). Here it is important to note that electronegativity is described as the negative of chemical potential (Pearson and Am 1963; Pearson 1963; Parr et.al. 1999; Koopmans 1934).

$$\chi = -\mu = 1 + A/2 \text{ -----1}$$

$$= 1 - A/2 \text{ -----2}$$

Softness (σ) that is a measure of the polarisability of chemical species is defined as the multiplicative inverse of chemical hardness ($\sigma = 1/\chi$). Electrophilicity (ω) and nucleophilicity are two useful chemical reactivity indices. Parr who made many studies on chemical reactivity proposed the

following formula to calculate the electrophilicity index depending on electronegativity and hardness values of chemical species. In addition, he described the nucleophilicity (ν) as the multiplicative inverse of electrophilicity ($\nu = 1/\omega$)

$$\omega = \chi^2/2 \text{ -----3}$$

$$\chi = (E_{\text{HOMO}} + E_{\text{LUMO}})/2 \text{ -----4}$$

$$= (E_{\text{HOMO}} - E_{\text{LUMO}})/2 \text{ -----5}$$

The energies of the highest occupied molecular orbital (HOMO) and the lowest unoccupied molecular orbital (LUMO) are computed at various

level. The HOMO-LUMO energy gap reveals the intra-molecular charge transfer (ICT) interaction occurs within the molecule.

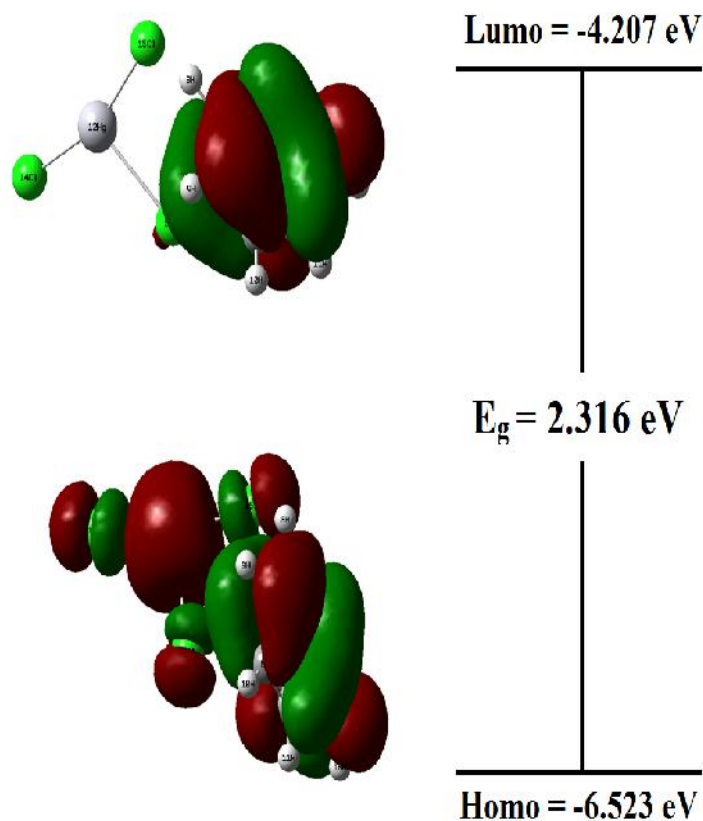


Figure 7. HOMO and LUMO plot of the crystal

The frontier molecular orbitals play an important role in the optical and electric properties, quantum chemistry and UV-visible spectra. The chemical stability of the molecule also depends on the nature of the frontier orbitals. The HOMO represents the ability to donate an electron and LUMO as an electron acceptor represents the ability to accept an electron, whereas dealing with molecular orbitals interaction, the two orbitals (HOMO and LUMO) of the crystal (Gandhimathi et. al. 2018). The energies of HOMO, LUMO and the orbital energy

gaps are calculated to assess the energetic behaviour of the molecule. The figure representation of HOMO and LUMO are shown in Figure 6. The calculated HOMO and LUMO energy values in the gas phase for the mentioned compound were -6.523 eV and -4.207 eV respectively, and the frontier orbital energy gap value was 2.316 eV. The narrow energy gap between HOMO and LUMO facilitated intramolecular charge transfer, which made the material NLO active.

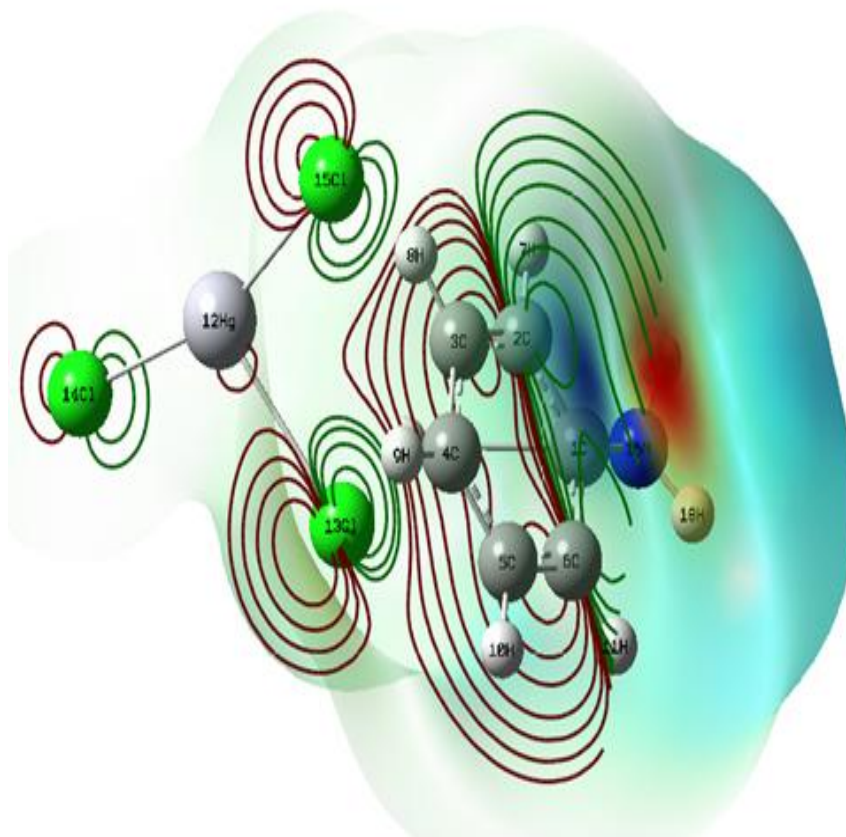


Figure 8. Molecular electrostatic potential surfaces of the crystal

The electrostatic potential surface of ATG-Hg molecule is shown in Figure 7. Different colour codes are used in electrostatic maps to identify different electron density sites in various parts of the molecule. The maximum negative potential (yellow region) is located on 15N and 18H of the amine group and 2C and 7H of hydrocarbon group, which right side to amine group showing their massive electron density which is responsible for its affinity towards the protons. The sky blue region mostly covers the hydrogen atoms of the NH₂ groups which indicate us to know the electrophilic nature of the amine group in the anionic moiety. The MEP surface shows that the reactivity against positive or negative reactants and attributes structure-activity relation of the system (Al-Omary et. al. 2015). There exists a correlation between electrostatic potential and the dipole moment, electronegativity and partial charges (Devi et.al. 2018)

3.8 Antimicrobial activity studies

A small amount (about µg) of the grown crystal weighed and dissolved in 1 ml of DMSO solvent to obtain stock solutions. The diameter zones were measured which exhibit the growth of tested microorganism. The crystal showed excellent microbial activities against various bacterial and fungal strains.

3.8.1 Antibacterial activity study

Antibacterial in vitro study, the bacterial species *Staphylococcus aureus* (Lab isolate), *Escheria coli*, *Pseudomonas aeruginosa*, *Staphylococcus epidermidis*, *Staphylococcus aureus* (Clinical isolate), *Enterococcus faecalis*, were prepared at a concentration of 100 µg/ml and Tetraglycine was used as a standard drug for the comparison of bacterial results and the results obtained are given

in Table 2. From the data, it is found that the crystal shows good exhibition activity against *Staphylococcus aureus* (Lab isolate), *Esheria coli*, *Speudomonas sp.*, *Staphylococcus epidermidis* and bacteria species and the crystal shows marked good exhibition activity against *Staphylococcus aureus* (Clinical isolate), *Ptoteus sp.* and *Speudomonas sp* bacteria species. The synthesized crystal shows no good exhibition activity against *Enterococcus faccalis* bacteria specie.

3.8.2 Antifungal activity study

The antifungal activity of the crystal was measured using Nystatin as a standard drug for the comparison of antifungal results. The antifungal

exhibition activity results of the crystal are given in Table 3. From the data, it is observed that the crystal shows good antifungal exhibition activity against *Aspergillus niger*, *Aspergillus flavus* and *Candidia albicans* and the grown crystal shows remarkable exhibition activity against *Penicillium sp* and the crystal shows no exhibition activity against *Aspergillus fumigates* fungal species. The antifungal data indicates that the synthesized crystal exhibits marked enhancement in the antifungal agent.

Table 2. Antibacterial activity of ATC-Hg crystal

Bacteria	ATC-Hg crystal	Tetraglycline
<i>Ptoteus sp.</i>	14	19
<i>Staphylococcus aureus</i> (Lab isolate)	21	20
<i>Esheria coli</i>	28	24
<i>Pseudomonas areuginosa</i>	27	23
<i>Speudomonas sp.</i>	19	22
<i>Staphylococcus epidermidis</i>	27	25
<i>Staphylococcus aureus</i> (Clinical isolate)	25	23
<i>Enterococcus faccalis</i>	-	24

Table 3. Antifungal activity of ATC-Hg crystal

Fungi	ATC-Hg crystal	Tetraglycline
<i>Aspergillus niger</i>	29	23
<i>Aspergillus flavus</i>	27	22
<i>Penicillium sp.</i>	18	21
<i>Candidia albicans</i>	31	23
<i>Aspergillus fumigatus</i>	-	22

4. Conclusions

Anilinium trichloromercurte(II) was grown from aqueous solution by slow solvent evaporation method at room temperature. The grown crystals were characterized by using CHNS, PXRD, thermal, spectral and second order nonlinear optical properties. The elemental analysis of the material

confirms the formation of the compound in stoichiometric ratio. While the powder XRD pattern confirms the crystallinity of the compound, the TG thermogram confirms its stoichiometry. The UV-Vis-NIR spectroscopic study revealed that the grown crystal has good optical transmittance and shows that the grown crystal suitable for the

optoelectronic applications. A fitting decomposition pattern was formulated by using TG-DTA analysis. The thermal hysteresis found in heating and cooling curves in DSC analysis show that the compound exhibits first phase transition. The mode of stretching vibrations of different molecular groups present in the crystal was identified by FTIR spectral study. The SHG efficiency of the grown crystal studied using modified Kurtz-Perry powder technique and indicated that the material has SHG efficiency was half that of standard potassium dihydrogen phosphates. The grown crystal exhibits good antibacterial and antifungal activities. The DFT calculation study was studied to find out the HOMO-LUMO energy gap and intra-molecular charge transfer (ICT) interaction occurs within the molecule.


Acknowledgments

The authors acknowledge the services of Sophisticated Test and Instrumentation Centre, Cochin University of Science and Technology, Cochin, Indian Institute of Science, Bangaluru, IIT, Madras and SRMV College of Arts and Science, Coimbatore for their instrumental facilities. The one of the author (T.Dhanabal) also acknowledge the Chairman and Secretary of Muthayammal College of Engineering, Rasipuram, Tamil Nadu, India for their constant encouragement and support. The one of the author (G.Raja) also acknowledge the Chairman and Secretary of Paavai Engineering College (Autonomous), Paachal, Rasipuram, Tamil Nadu, India for their constant encouragement and support.

References

- [1] J.T. Lin, V.S. Wang, H. Arend, SPIE 1104 (1989) 100-132.
- [2] U. Duo-rong, X.U. Dong, Z.L. Nan, I.U. Ming-guo, J. Min-hua, Chin. Phys. Lett. 13 (1996) 841-843.
- [3] S. Masilamani, P. Ilayabarathi, P. Maadeswaran, J. Chandrasekaran, K. Tamilarasan, Optik 123 (2012) 1304–1306.
- [4] D.S. Chemla, J. Zyss, Acta Polym. 39 (12) (1987) 726-727.
- [5] P.R. Newman, L.F. Warren, P. Chunningham, T.V. Chang, D.E. Copper, G.L. Burdge, P. Polak-Dingles, C.K. Lowe-ma, Mat. Res. Sol. Sym. Proc. 173 (1990) 557-561.
- [6] Amitav Malik, R.R Dayal, International Conference on Laser Materials and devices edited by BP (31) 1999.
- [7] J. Johnson, R. Srineevasan, D. Sivavishnu, Materials Science for Energy Technologies 2 (2019) 226-233.
- [8] J. Kennedy, P.P. Murmu, E. Manikandan, S.Y. Lee, J. Alloy. Compd. 616 (2014) 614-617.
- [9] A. Hemalatha, S. Arulmani, K. Deepa, D. Suresh Kumar, J. Madavan, S. Senthil, Mater. Today. Proc. 8 (2019) 142-147.
- [10] N. Indumathi, A. Hemalatha, E. Chinnasamy, A. Venkatesan, M.E. Raja Saravanan, K. Deepa, P. Matheswaran, S. Senthil, K. Kaviyarasu, R. Uthrakumar, Materials Today: Proceedings 36 (2021) 150-154.
- [11] T. Pal, T. Kar, X.-Q. Wang, G.-Y. Zhou, D. Wang, X.-F. Cheng, Z.-H. Yang, J. Cryst. Growth 235 (2002) 523-528.
- [12] P. Anwar, S. Okada, H. Oikawa, H. Nakanishi, Chem. Mater. 12 (2000)1162-1170.
- [13] L. Guru Prasad, V. Krishnakumar, G. Shanmugam, R. Nagalakshmi, Structural, thermal and optical studies on 2-naphthol crystals, Cryst. Res. Technol. 45 (2010) 1057–1063.
- [14] M. Vimalan, T. Rajesh Kumar, S. Tamilselven, P. Sagayaraj, C.K. Mahadevan, Physica B 405 (2010) 3907-3913.
- [15] S.K. Kurtz, T.T. Perry, J. App. Phy. 39 (1968) 3798-3813.
- [16] R. G. Pearson, J. Am. Chem. Soc. 85 (1963) 3533-3539.
- [17] R. G. Pearson, Inorg. Chem. 27 (1988) 734-740.
- [18] R. G. Parr, L.V. Szentpaly, S. Liu, J. Am. Chem. Soc. 121 (1999) 1922-1924.
- [19] T. Koopmans, Physica, 1 (1934) 104-113.
- [20] A. Gandhimathi, R.T.Karunakaran, A.Elakkinna Kumaran, S. Prabahar, Opt. Laser Technol. 103 (2018) 291-299.
- [21] F. A. M. Al-Omary, Y. Sheena Mary, C. Yohannan Panicker Ali, A. El-Emam Ibrahim, A. Al-Swaidan Abdulaziz, A. Al-Saadi, C. Van Alsenoy, J. Mol. Struct. 1096 (2015) 1-14.

- [22] J. Devi, M. Yadav, D. Kumar, L. S. Naik, D.K. Jindal, Appl. Organomet. Chem. 33 (2018) 1-10.

Access this Article in Online	
	Website: www.ijcreps.com
	Subject: Chemistry
Quick Response Code	
DOI: 10.22192/ijcreps.2023.10.11.001	

How to cite this article:

G.Raja and T.Dhanabal. (2023). Growth, spectral and thermal characterization of anilinium trichloromercurate(II) crystal. Int. J. Curr. Res. Chem. Pharm. Sci. 10(11): 1-13.

DOI: <http://dx.doi.org/10.22192/ijcreps.2023.10.11.001>